ANTIPODAL VIVALDI ANTENNA PERFORMANCE BOOSTER EXPLOITING SNUG-IN NEGATIVE INDEX METAMATERIAL

A. R. H. Alhawari[1], A. Ismail[1, 2, *], M. A. Mahdi[1], and R. S. A. R. Abdullah[1]

[1]Centre of Excellence for Wireless and Photonics Network, Department of Computer and Communication Systems Engineering, Faculty of Engineering, Universiti Putra Malaysia, Malaysia

[2]Institute of Advanced Technology, Universiti Putra Malaysia, Malaysia

Abstract—Despite its popularity, the conventional Vivaldi antenna has long suffered from some design problems, such as tilted beam, low or inconsistent directivity and gain, complicated design and fabrication methods, and limited size reduction. These setbacks make its progress lag on the fast track of technological demand. Thus, the antenna overall performance is anticipated to improve by incorporating negative index metamaterial (NIM) into the design method, plus, it is also tunable. In this study, the design uses linearly-tapered shape-loading structure, as its projected performance crucially depends on the space in between the antenna arms, a prerequisite to further boost its performance when combined with NIM technology. A unique slitting approach synchronizes the integration between the Vivaldi antenna and NIM where a single layer NIM piece is simply snugged into the slit perpendicular to the middle antenna substrate. The major improvement in the spotlight is the capability of NIM to focus the entire beam so that it can radiate to the targeted direction. The measurement results are similar to the simulations in terms of high gain, where the gain and directivity of the antenna are increased up to 4 dB. The contrast of overall performance between the plain modified Vivaldi antenna and the ones with NIM evidently asserts the expected contribution of snug and boost method applied and attests its significant potentials for a broad range of ultra-wideband applications.

1. INTRODUCTION

In 1979, Gibson in his work [1] proposed a new class of antenna known as Vivaldi antenna. And to date, this type of antenna is the most widely used in many applications for instance microwave imaging, see-through-wall (STW), phase array systems, and UWB systems, etc. The main reason for its reputation is due to their set of more favorable distinctive characteristics than other types of wideband antennas, including planar and simple structure, light weight, compactness, ultra-wideband, high efficiency, moderate gain and directivity, and symmetric beam in E-plane and H-plane. Moreover, it is among the most economical methods to fabricate using common printed circuit board (PCB) technology and easy to be integrated with other microwave components.

Theoretically, Vivaldi antenna has infinite bandwidth [1], and in general, the bandwidth is proportional to its length and aperture. Consequently, the size of the antenna increases when augmentation of UWB performance is required. Another issue is on miniaturization; in spite of various antipodal Vivaldi antenna (AVA) designs attempted to attain more compact size [2–7], yet, they are found inevitably limiting directivity and stability of radiation patterns. In order to overcome the directivity and gain flaws of Vivaldi antenna, different approaches have been introduced in [8, 9] using array of Vivaldi antennas. Unfortunately, it also contributes the challenges of size, apart from the fact that it complicates the fabrication method, thus, adds the overall cost and demands extra efforts.

Recently, a new approach was introduced in [10] to improve the AVA directivity by inserting a '*director*' — a uniquely shaped material of a higher dielectric constant material into the aperture. Another technique reported in [11] is applying elongation technique to the antenna substrate beyond its aperture. The designs both produce high gain and directivity within a wide frequency band. Other current work by Zhou and Cui [12] and Zhou et al. [13] in 2011 incorporated zero-index metamaterials (ZIM) into Vivaldi antenna in an effort to enhance its directivity and gain by integrating the single-layer and multi-layer into the Vivaldi antenna. Regrettably, the narrow bandwidth of ZIM again limits the directivity and gain consistency of the Vivaldi antenna. Eventually, the idea defied the required goal of miniaturization since higher directivity means more layers of ZIM applied. These drawbacks inexorably necessitate another conquering endeavor that harmoniously neutralizes the co-existence of compactness, high directivity and gain along with simplicity and flexibility in design method at the lowest possible cost. Briefly, enhancing design techniques using metamaterial

are still challenging the circuit designers.

This paper is dedicated to the incorporation of an improved NIM in [14] into a modified AVA aiming to boost its directivity and gain, together with superior beam focus efficiency at the least possible size and cost. Being flexible, the size of the AVA may stay similar or increased in length from the attachment of the NIM. It depends on the required length of the NIM and the type of application in use. Nevertheless, its offer of compactness and design flexibility remains intact. Both simulated and measured results of the proposed AVA with and without NIM are presented and contrasted.

2. THE MODIFIED AVA DESIGN

Referring to $[1, 6, 7, 12]$ for AVA designs, the radiator patch and the ground plane of the proposed antenna were developed with linearly-tapered shape, and microstrip line is used to feed it. The top surface of the substrate has the left arm (radiator patch) of the antenna, while the bottom surface has the right arm (ground plane). The main advantages of this design over the ordinary AVA designs is that it has higher performance characteristics in terms bandwidth, gain, directivity, radiation pattern, angular width, and radiation efficiency at compact size. The geometry and photograph of the proposed AVA is depicted in Figure 1, and its geometrical parameters are given in Table 1. The proposed antenna was fabricated on a 0.787 mm thick Rogers RT/Duroid 5880 substrate with a dielectric constant of 2.2 and loss tangent of 0.0009.

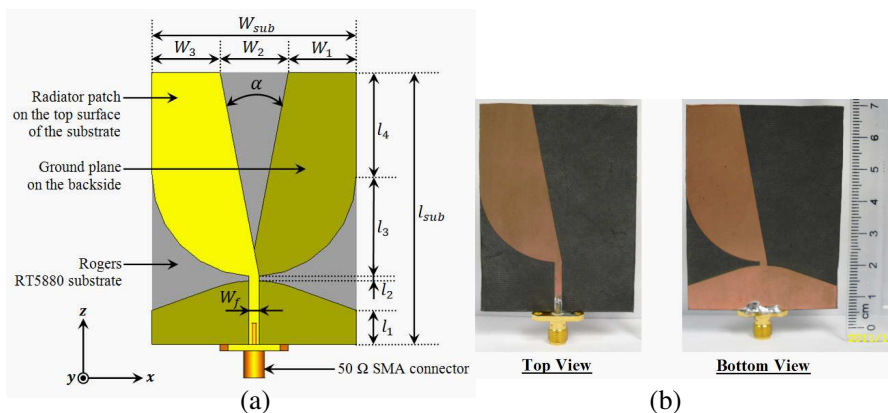Figure 2 shows the simulated return loss result for the antenna for

Figure 1. (a) Antenna geometry and (b) photograph.

Table 1. Final antenna parameters design.

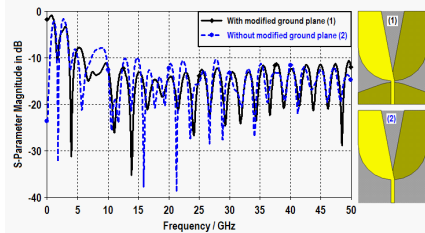| Parameter	l_1	l_2	l_3	l_4	l_{sub}	W_1	W_2	W_3	W_f	W_{sub}
Dimension (mm)	8	1	24	24	64	16	16	16	2.4	48

Figure 2. Return loss result of the proposed antenna with and without modified ground plane.
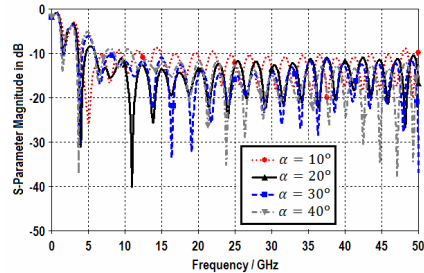

Figure 3. Simulated return loss of the proposed AVA for different values of α.

two different cases: with modified ground plane and without modified ground plane, using full-wave electromagnetic simulation [15]. The curve in the figure indicates that the former performs better than the latter. Figure 3 shows our stimulations with four different variables of value distancing between the radiator patch on the top surface of the substrate and the ground plane on the backside, labeled by (α), as shown in Figure 1(a) to see the influence on return loss. The figure distinguishes the values that work best with the design, which is between (20°–30°) only. So, it can be concluded from Figure 3 that the choice of α value is critical to achieving broader bandwidth and better return loss, i.e., below -10 dB.

3. THE AVA INCORPORATED WITH NIM

3.1. NIM Structure

The NIM structure shown in Figure 4 seems to fit efficiently and smoothly well with the modified AVA; more details about the NIM design are provided in [14]. The NIM unit cell with dimensions of $A = B = 8$ mm is designed on an identical substrate material used for the AVA design. The NIM is excited with an electric field along the y-direction and a magnetic field along x-direction as illustrated in
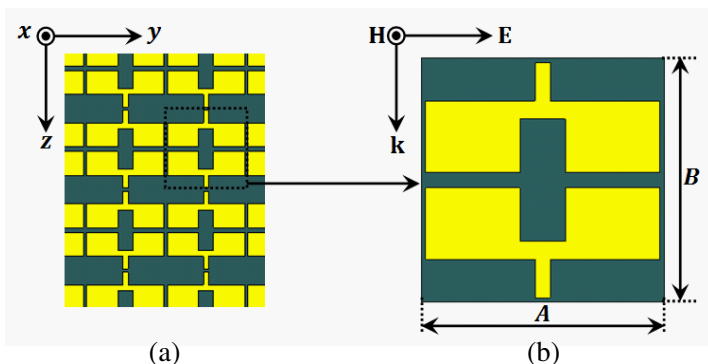
(a)   (b)

Figure 4. (a) NIM configuration and (b) its unit cell [14].
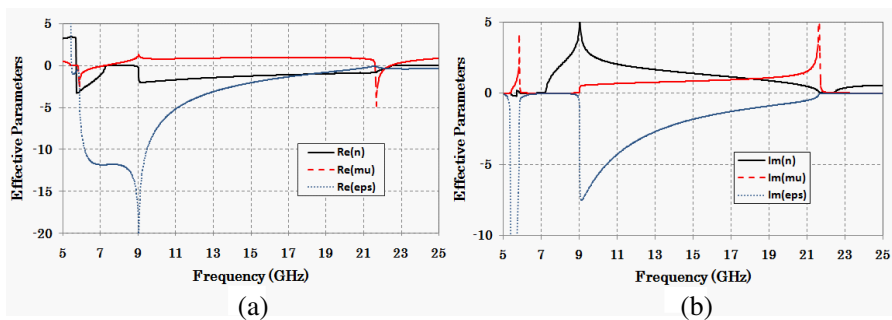

(a)   (b)

Figure 5. Retrieved effective parameters, (a) real parts and (b) imaginary parts.

Figure 4. Effective constitutive workable parameters were obtained via retrieval algorithm described in [16, 17], and the results are shown in Figure 5.

From Figure 5(a), the extracted real part of the permeability μ is simultaneously negative over two narrow frequency bands, 5.79–7.18 GHz and 21.6–22.68 GHz, respectively. The effective permittivity ε is negative over a broad band from 5.5–21.04 GHz. The metamaterial unit cell structure exhibits two left-handed passbands at the overlapped region where ε and μ are simultaneously negative, and the corresponding values of the negative refractive index n are 5.7–7.27 GHz and 8.9–22.68 GHz, respectively. Hence, this metamaterial type validates its privileges especially where higher directivity and gain of Vivaldi antenna over wideband of frequency is the main target.

3.2. NIM Incorporated AVA

In order to distinctively differ from other existing techniques of incorporating the improved NIM into the modified AVA, our unique approach is characterized by '*slitting*' the mid-section of the antenna substrate specifically in between the two arms of the antenna. The dimensions of the slit need to be precisely fit a single layer of the NIM alone. It is purposely to maintain similar return loss results (below $-10\,\text{dB}$) as found in the 'without slit' design as illustrated in Figure 6. The length of the slit is $32\,\text{mm}$ while its width is $0.787\,\text{mm}$. The application of these particular slit dimensions does not significantly affect the simulated return loss results of the antenna, which are luckily
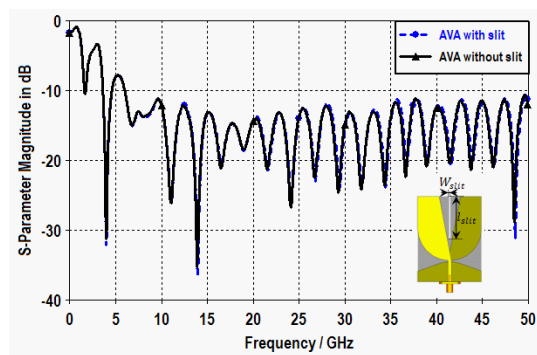

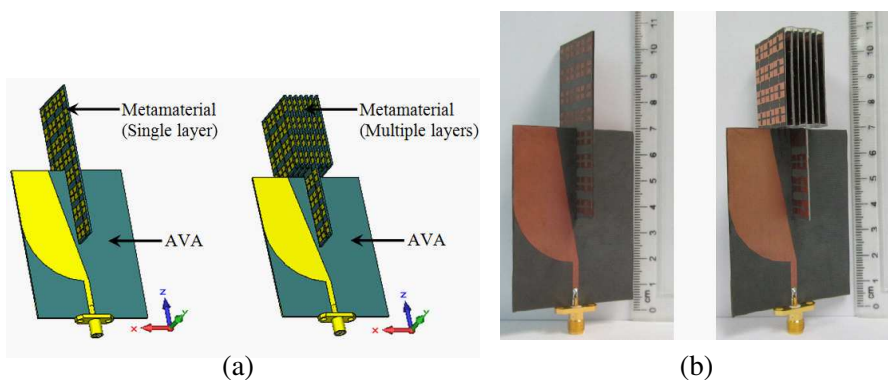**Figure 6.** Simulated return loss of the modified AVA with and without slit.

Figure 7. (a) The proposed AVA incorporated with NIM and (b) photograph.

similar to the one without slit as shown in Figure 6. In order to enhance the directivity of the AVA at other alternative frequencies, we simply alter the NIM characteristics accordingly. Additionally, it is also easily applicable into any other type of NIM, which operates within AVA operating frequency, i.e., the design technique grants more freedom to a designer depending on one's required application. This design flexibility will benefit miniaturization objective along with the NIM technology trend in the industry.

As shown in Figure 7, a single layer and multiple layers NIMs were assembled into the modified AVA, whereby all use identical type of substrate to further promote economical aim. Figure 7 demonstrates that the single layer NIM piece is simply snugged into the slit perpendicular to the middle substrate of AVA. The snug method simplifies the fabrication of the single layer NIM AVA a lot. The same goes to the multiple layers NIM AVA design. What differs between the single layer and multiple layers NIMs is the attachment of the latter to both sides of the single layer, specifically behind the aperture on a single slit. It is crucial that the additional NIM layers are to be attached only in between the antenna arms as simulation results recommended that the final width of the NIM should be less than or equal to the distance between the antenna arms (W_2) in order to boost the AVA performance. Accordingly, the space between the NIM layers attached must equal to 1.6 mm each. In addition to simplification of fabrication, it also contributes flexible idea or method to significantly improve the antenna performance with compact size. The simulated results of the return loss for the AVA with and without NIM are illustrated in Figure 8.
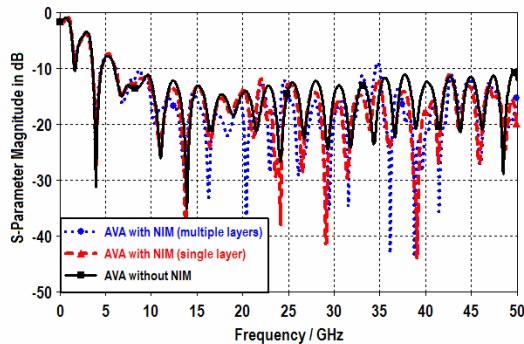

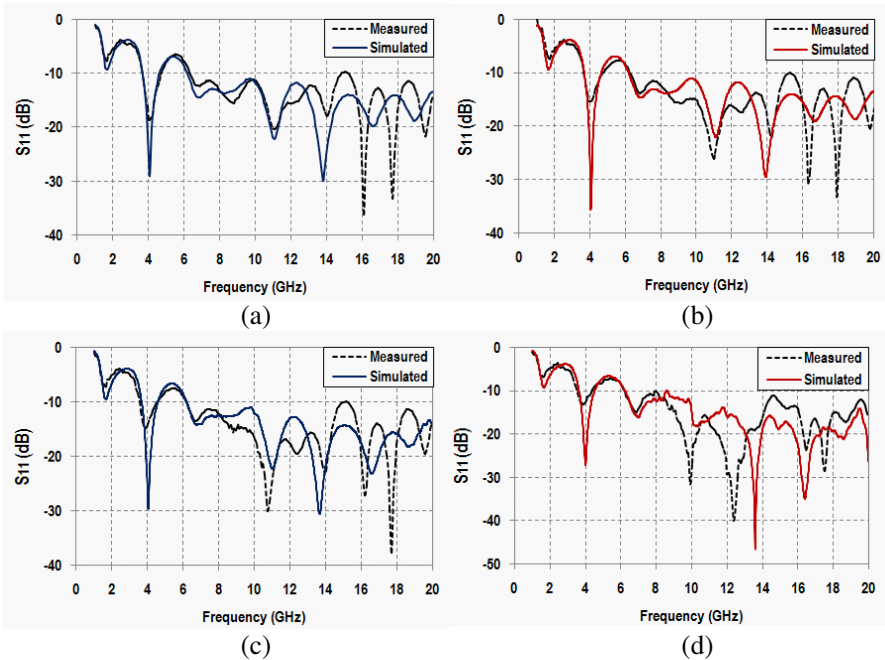**Figure 8.** Simulated return loss of the AVA with and without NIM.

Figure 9. Measured and simulated return loss of the modified AVA:
(a) without slit and NIM, (b) with slit, (c) with NIM (single layer),
and (d) with NIM (multiple layers).

4. RESULTS AND DISCUSSION

The capability of the NIM to enhance the performance of the AVA,
both with and without NIM, was verified using CST Microwave Studio
Simulator [15], and the measurements were carried out via an Anritsu
37347D vector network analyzer (VNA). The results are depicted in
Figures 9(a)–(d). The overall results show that the antenna with
NIM performs better than the one without NIM, where S_{11} is below
-10 dB between 6 to 20 GHz (the maximum VNA frequency provided).
Specifically, the best performance is certainly achievable using multiple
layers NIM. Notwithstanding, the ultra-wide bandwidth performance
of the AVA is consistent whether using single layer or multiple layers
of the NIM, where the return loss is better reduced to below -10 dB.
The slight difference between the measured and simulated results is
originated from the mismatch between the feeding line and SMA
connector, as well as the inevitable defect of PCB fabrication process,
which were void in the simulation, e.g., exact symmetrical alignment

of the multiple layers.

As shown in Figures 10(a)–(c), the gain and directivity of the antenna have been greatly improved by the NIM especially when the multiple layers are used in the frequency band from 9 GHz to 20 GHz,
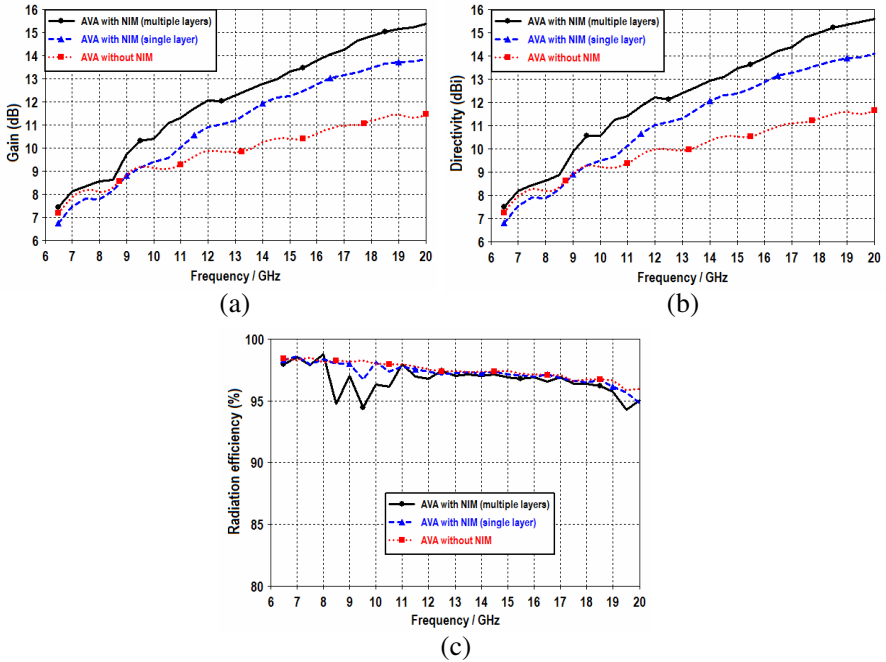

Figure 10. Simulated (a) gain, (b) directivity, and (c) radiation efficiency.
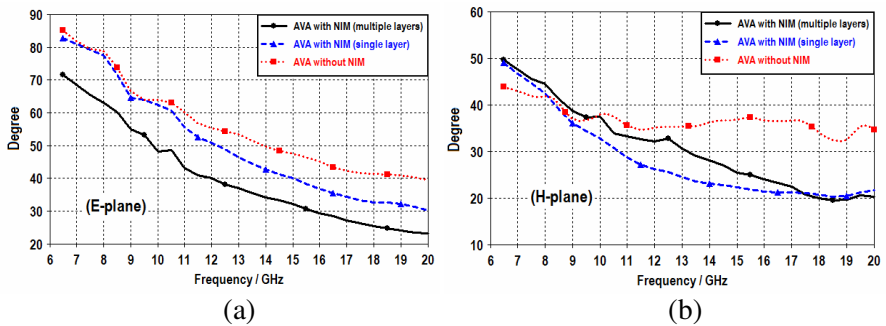

Figure 11. Simulated (a) angular width (*E*-plane), and (b) angular width (*H*-plane).

where the band of the negative index of refraction for the NIM exists. Overall, all types of the examined antennas show higher gain and directivity when simulated with higher frequencies where at least 94%

Table 2. Comparison of E-plane peak gain and HPBW antennas performance.

| Frequency (GHz)	E-plane peak gain (dB)			E-plane HPBW and (main lobe direction)		
	Original	Single layer	Multiple layers	Original	Single layer	Multiple layers
6.5	7.18	6.76	7.42	85.6° (−1°)	83.1° (10°)	71.7° (2°)
7	7.88	7.48	8.10	82.2° (−1°)	81.2° (−11°)	68.7° (0°)
9	8.86	8.82	9.74	66.9° (0°)	64.9° (0°)	55.3° (0°)
10	9.15	9.46	10.40	64.3° (−1°)	62.8° (−2°)	48.5° (0°)
11	9.30	10.00	11.30	60.4° (−1°)	55.9° (−1°)	43.6° (0°)
12	9.88	10.90	12.10	55.7° (−1°)	51.0° (−1°)	40.2° (0°)
13	9.81	11.20	12.30	53.7° (−1°)	46.7° (−1°)	37.4° (0°)
14	10.20	11.90	12.80	49.9° (0°)	43.1° (0°)	34.4° (0°)
15	10.40	12.30	13.30	47.8° (−1°)	40.2° (−1°)	32.7° (0°)
16	10.60	12.80	13.80	45.4° (−1°)	37.1° (0°)	29.5° (0°)
17	11.00	13.10	14.30	42.7° (0°)	34.8° (0°)	27.6° (0°)
18	11.20	13.50	14.90	41.6° (0°)	33.0° (0°)	26.1° (0°)
19	11.50	13.70	15.10	41.2° (0°)	32.6° (0°)	24.7° (0°)
20	11.50	13.90	15.40	39.6° (0°)	30.3° (0°)	23.9° (0°)

radiation efficiency yielded. Comparing the AVA (without NIM) with the new AVA with single layer NIM and AVA with multiple layers NIM, the results demonstrate gain increment up to 2.5 dB, and 4 dB, respectively.

In Figure 11, the angular widths in both E- and H-planes as a function of frequency are shown as well. Table 2 serves to better clarify our comprehension on improved performance of those antennas: the simulated E-plane peak gain, half-power beamwidth (HPBW), and main lobe direction within the frequency band from 6.5 GHz to 20 GHz. Obviously, Table 2 highlights the advantages of using NIM particularly when multiple layers are applied that it is more capable to focus the radiation patterns to the targeted direction. As can be observed from Table 2, the HPBW of the new AVA with NIM (single layer) decreases about 10 degrees, compared to the AVA without NIM. Meanwhile, the AVA with NIM (multiple layers) decreases about 20 degrees.

Figure 12 plots both E- and H-plane radiation patterns of the
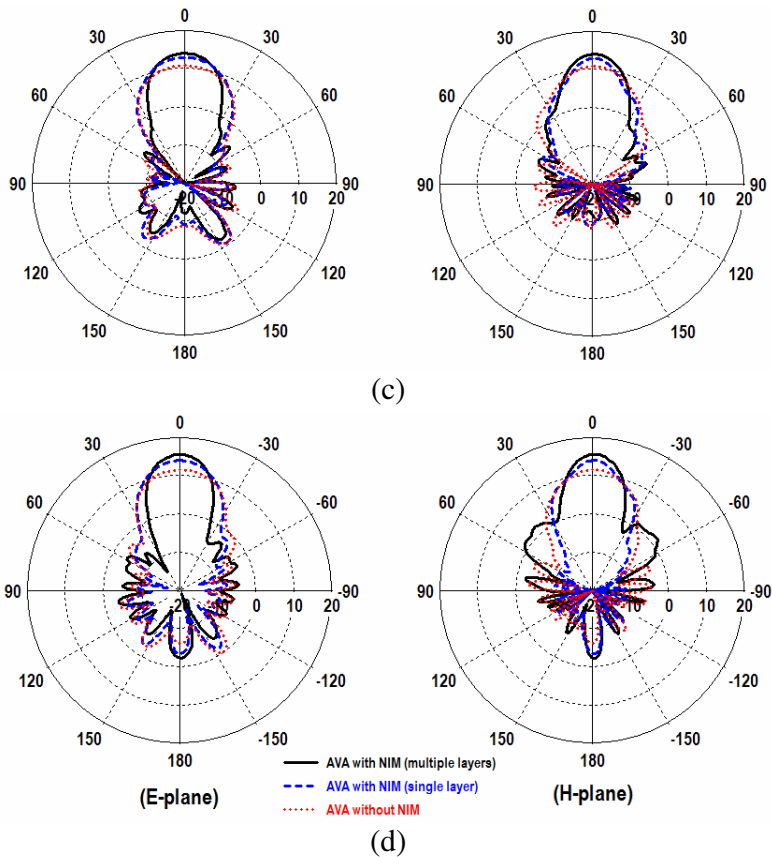

(a)

(b)

(c)

(d)

(E-plane)   (H-plane)

AVA with NIM (multiple layers)
AVA with NIM (single layer)
AVA without NIM
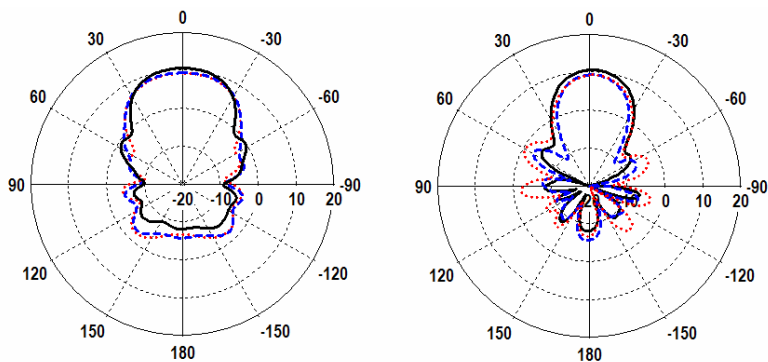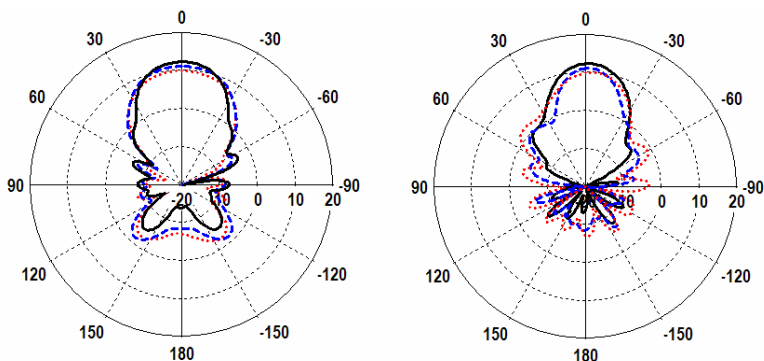
Figure 12. Comparison for simulated E-plane (x-z) and H-plane (y-z) radiation patterns of the antennas at: (a) 9.5 GHz, (b) 12 GHz, (c) 16 GHz, and (d) 19.5 GHz.

modified AVA, single layer NIM and multiple layers NIM AVA at 9.5, 12, 16, and 19.5 GHz, respectively. As revealed by the results, the multiple layers NIM AVA shows more significant anticipated improvement in directivity than the antenna without or with single layer NIM. All the antennas also exhibit almost symmetrical radiation patterns in both the E- and H-planes. Figure 13 shows the simulated co- and cross-polarization far field radiation patterns of the proposed NIM AVA (multiple layers) for both planes. The plots illustrate low cross-polarization levels of the designed antenna. The values of cross-polarization in the main lobe direction towards the co-polarization are better than -15 dB in E-plane and -20 dB in H-plane.
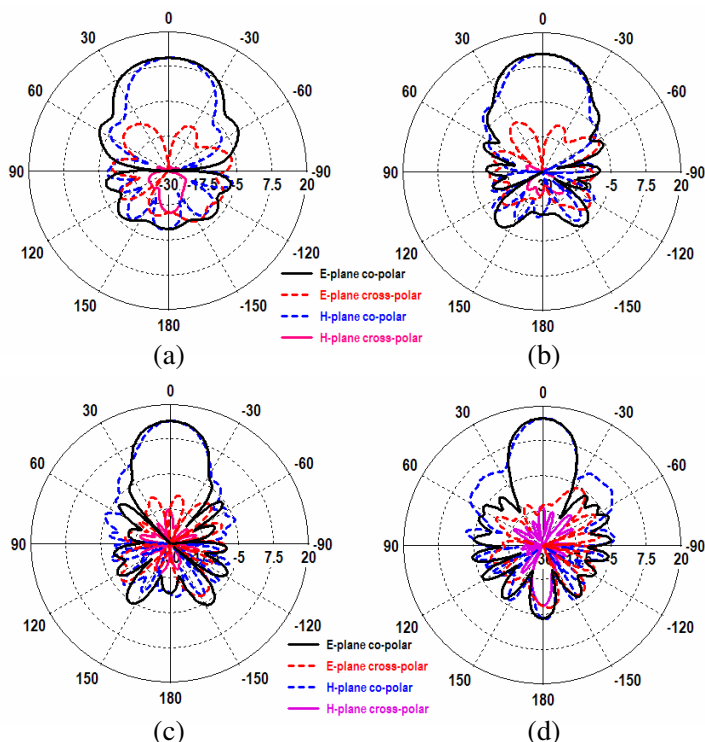
Figure 13. Simulated far field radiation patterns of the proposed AVA with NIM (multiple layers) at: (a) 9.5 GHz, (b) 12 GHz, (c) 16 GHz, and (d) 19.5 GHz.

5. CONCLUSION

The paper introduces an ingenious technique to boost the performance of the legendary Vivaldi antenna. The traditional AVA is modified using linearly-tapered shape-loading structure to easily integrate with single layer and multiple layers metamaterial. The NIM AVA exhibits significant enhancement in the gain and directivity as well as to correct the tilted radiation patterns especially for the multiple layers NIM AVA. It also exhibits almost symmetrical radiation patterns in both E- and H-planes as well as produces high gain varying from 7.42 to 15.4 dB in the frequency bandwidth of 6.5–20 GHz. The gain of the single layered NIM AVA increases approximately 2.5 dB while the HPBW decreases about 10 degrees, compared to the plain AVA. Interestingly, the multiple-layered NIM AVA performs better with increased gain up

to 4 dB, and its HPBW roughly decreases up to 20 degrees.

In summary, this antenna offers simplified flexible snug-in method integrating the modified AVA and NIM (or any other type of NIM) to boost directivity and gain, plus, narrower beam width in the E- and H-planes with lower cross-polarization within broader bandwidth with the least possible size and cost. Simulated and measured results of both proposed AVA with and without NIM are presented. This technology is exceptionally practical for UWB applications, for instance, see-through-wall imaging and breast tumor detection.

ACKNOWLEDGMENT

REFERENCES

1. Gibson, P. J., "The Vivaldi aerial," *9th European Microwave Conference*, 101–105, 1979.

2. Mehdipour, A., K. Mohammadpour-Aghdam, and R. Faraji-Dana, "Complete dispersion analysis of Vivaldi antenna for ultra wideband applications," *Progress In Electromagnetics Research*, Vol. 77, 85–96, 2007.

3. Wang, Z. and H. Zhang, "Improvements in a high gain UWB antenna with corrugated edges," *Progress In Electromagnetics Research C*, Vol. 6, 159–166, 2009.

4. Jolani, F., G. R. Dadashzadeh, M. Naser-Moghadasi, and A. M. Dadgarpour, "Design and optimization of compact balanced antipodal Vivaldi antenna," *Progress In Electromagnetics Research C*, Vol. 9, 183–192, 2009.

5. Bai, J., S. Shi, and D. W. Prather, "Modified compact antipodal Vivaldi antenna for 4–50 GHz UWB application," *IEEE Transactions on Microwave Theory and Techniques*, Vol. 59, 1051–1057, 2011.

6. Kota, K. and L. Shafai, "Gain and radiation pattern enhancement of balanced antipodal Vivaldi antenna," *Electronics Letters*, Vol. 47, 303–304, 2011.

7. Fei, P., Y. Jiao, W. Hu, and F. Zhang, "A miniaturized antipodal Vivaldi antenna with improved radiation characteristics," *IEEE Antennas and Wireless Propagation Letters*, Vol. 10, 127–130, 2011.

8. Yang, Y., Y. Wang, and A. E. Fathy, "Design of compact Vivaldi antenna arrays for UWB see through wall applications," *Progress In Electromagnetics Research*, Vol. 82, 401–418, 2008.

9. Lin, S., S. Yang, A. E. Fathy, and A. Elsherbini, "Development of a novel UWB Vivaldi antenna array using SIW technology," *Progress In Electromagnetics Research*, Vol. 90, 369–384, 2009.

10. Bourqui, J., M. Okoniewski, and E. C. Fear, "Balanced antipodal Vivaldi antenna with dielectric director for near-field microwave imaging," *IEEE Transactions on Antennas and Propagations*, Vol. 58, No. 7, 2318–2326, Jul. 2010.

11. Kota, K. and L. Shafai, "Gain and radiation pattern enhancement of balanced antipodal Vivaldi antenna," *Electronics Letters*, Vol. 47, No. 5, 303–304, 2011.

12. Zhou, B. and T. J. Cui, "Directivity enhancement to Vivaldi antennas using compactly anisotropic zero-index metamaterials," *IEEE Antennas and Wireless Propagation Letters*, Vol. 10, 326–329, 2011.

13. Zhou, B., H. Li, X. Zou, and T.-J. Cui, "Broadband and high-gain planar Vivaldi antennas based on inhomogeneous anisotropic zero-index metamaterials," *Progress In Electromagnetics Research*, Vol. 120, 235–247, 2011.

14. Alhawari, A. R. H., A. Ismail, M. A. Mahdi, and R. S. A. Raja Abdullah, "Development of novel tunable dual-band negative index metamaterial using open stub-loaded stepped-impedance resonator," *Progress In Electromagnetics Research B*, Vol. 35, 111–131, 2011.

15. Computer Simulation Technology (CST) Microwave Studio, 2010.

16. Chen, X., T. M. Grzegorczyk, B. I. Wu, J. Pacheco, and J. A. Kong, "Robust method to retrieve the constitutive effective parameters of metamaterials," *Physical Review E*, Vol. 70, 016608/1–016608/7, 2004.

17. Smith, D. R., D. C. Vier, T. Koschny, and C. Soukoulis, "Electromagnetic parameter retrieval from inhomogeneous metamaterials," *Physical Review E*, Vol. 71, 036617/1–036617/11, 2005.